Acoustic Emission in Bonded Elastomer Discs Subjected to Uniform Tension. II

P. A. KAKAVAS* and W. V. CHANG

Department of Chemical Engineering, University of Southern California, Los Angeles, California 90089

SYNOPSIS

The aim of this paper is to evaluate and analyze the growing and tearing mechanisms of existing microvoids within bonded elastomer discs using the acoustic emission (AE) technique. It was shown that the existing microvoids in the deformed disc are responsible for the reduction of the apparent modulus (M) of the elastomer disc, the stress softening, and the hysteresis when the material is subjected to triaxial stress conditions. A series of experiments performed in our laboratory confirmed the existence of microvoids within the deformed bonded unfilled nitrile rubber discs. Valuable information about the size of the deformed voids in the material was obtained using the frequency spectrum of the detected AE signals. More information on the tearing of voids was extracted from the count, event, amplitude, and duration time distribution of the received AE pulses.

INTRODUCTION

The basic structure of polymeric materials is different from metals, which results in differences in their fracture behavior. A review of the fracture in metals has been given by Williams.[1] Due to the expanding usage of polymers in engineering applications, a widespread interest in fracture properties has arisen. One prime example is the structural integrity of elastomers. Thus the motive for the investigation of fracture in hydrostatic tension is twofold: (a) to attempt to study failure in solid polymeric materials (e.g., elastomers) in order to discover the fundamental physical phenomena that occur and (b) to supply a sound basis upon which the fracture analysis of engineering components subjected to multiaxial stress states can be made with confidence. Investigation in the area of triaxial fracture has been limited. One of the first efforts in this direction was made by Gent and Lindley,[2,3] who performed tests in hydrostatic tension and compression.

They pursued experiments by manufacturing some small circular discs from a carbon back-filled natural rubber and pulled them by means of two rigid steel plates (see Fig. 1). Gent and Lindley's initial work demonstrated an internal fracture in the rubber which varied with thickness, modulus, and tensile strength, and they devoted their attention to documenting and explaining this variation. Emphasis was placed on defining the load–deflection relation and obtaining a definition of the stress field in the specimen. The work of Gent and Lindley was used as a point of departure for the work of Lindsey, Schapery, Williams, Zak, and Blatz at CALTECH.[4-7] The stress field, within a poker chip sample, was analytically estimated by Williams and Schapery,[6] in terms of modified Bessel functions and the aspect ratio (radius to thickness) of the sample.

Several years later, Chang and co-workers[8] investigated the fracture in carbon-black-filled rubber disks using the electron microscope. At the end of each test, they opened the poker chip and looked at the final structure of the testing material. Actually, a large number of microcavities were observed within the matrix of the rubber disk. Photographs of the voids in the deformed material were detected in Ref. 8. Gent and Tompkins have also reported additional information on the nuclentanion growth of gas bubbles in elastomer.[9]

In the first part[10] of these series of papers we have investigated the microcavitation in unfilled

* To whom the correspondence should be addressed at 135 Korinthou Street, 262 23 Patras, Greece.

Journal of Applied Polymer Science, Vol. 42, 1997–2004 (1991)

 CCC 0021-8995/91/071997-08$04.00

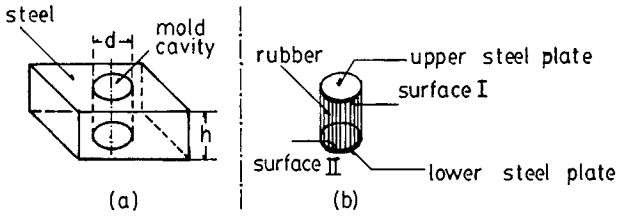

Figure 1 (a) The mold used for the preparation of the samples; (b) a poker chip specimen.

rubber disks subjected to hydrostatic compression using the *nonstructive* experimental method, the so-called acoustic emission (AE). In this article we investigate the microcavitation in rubber disks (poker-chip) subjected to hydrostatic tension using the AE technique.

The standard definitions of the acoustic emission terms, according to ASTM are reported in the section after eq. (4). In the next section, we report some experimental data of the (AE) response pulses and their frequency spectrum from the tension data. Regarding the AE phenomena as an explosion within an infinite elastic medium, we report a mathematical equation for the displacement field $u_r(r, t)$. The proposed equation involves three important factors: (1) the dumping coefficient α, (2) the size of the acoustic voids b, and (3) the frequency of the waveform ω, which are correlated throughout three mathematical equations.

In the section following eqs. (8), we report more AE data as the total number of AE events and counts as a function of the elapsed time of deformation.

We also report data on the event and count average rate as a function of the elapsed time. The total counts versus the applied load is given in the same section too. Experimental data on the normalized and cumulative amplitude distribution are reported on the poker-chip experiments.

EXPERIMENTAL

Materials

The chemical composition of the material used for this study is given in Table I, of Ref. 10. All the ingredients described in Table I were well mixed in an open two roll mill. Several pairs of cylindrical steel plates were sand-blasted and were well cleaned by a suitable solvent. A primer-coated (chemlock 205) was sprayed on the lower (surface I) and the upper (surface II) surfaces of the top and the bottom metal plates (see Fig. 1). The metal plates with the primer coat were left overnight to dry at room temperature. A bonding agent (chemlock 250) was sprayed on the top of primer-coated and the plates were dried for several hours. Thin cylindrical rubber sheets were cut from the mixed batch of the material and were placed between the metal plates (see Fig. 1). The whole sample was placed into the mold cavity for curing. The thickness of the samples was varied from 0.580 to 1.27 cm. The radius of the mold cavity was kept constant, for all the prepared samples, at $a = 7.62$ cm. The inside surface of the mold was sprayed with silicon mold release to ease the removal of the bonded rubber discs, after curing.

In order to estimate the minimal curing time of the compound the *curemeter curve* was obtained from the Mooney rheometer. Figure 2 shows the curemeter curve for the used material for this study. The curve indicates a minimal curing time of 4.5 min. The prepared samples of rubber disc were cured at $T_c = 370°F$, $P_c = 11.032\ N/mm^2$, and $t_c = 45$ min. The long curing time was selected to give sufficient time for temperature in the rubber disc to reach the curing temperature. At the end of the curing time, the pressure was released and the sample was taken away from the pressure machine to return to room conditions. Hereafter, these type of samples will be called poker chips. The prepared poker chips were pulled at constant strain rate ($v_p = 0.0254$ cm/min) in an MTS machine.

STRESS–STRAIN CURVE OF A BONDED ELASTOMER DISC SUBJECTED TO UNIFORM TENSION

The response of a poker chip sample (sample #6) is shown in Figure 3. The sample was pulled, on an

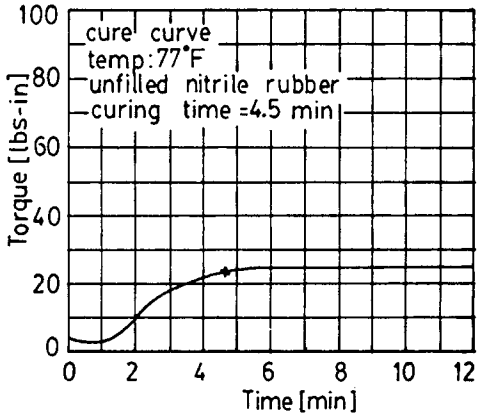

Figure 2 Curemeter curve from an unfilled nitrile rubber.

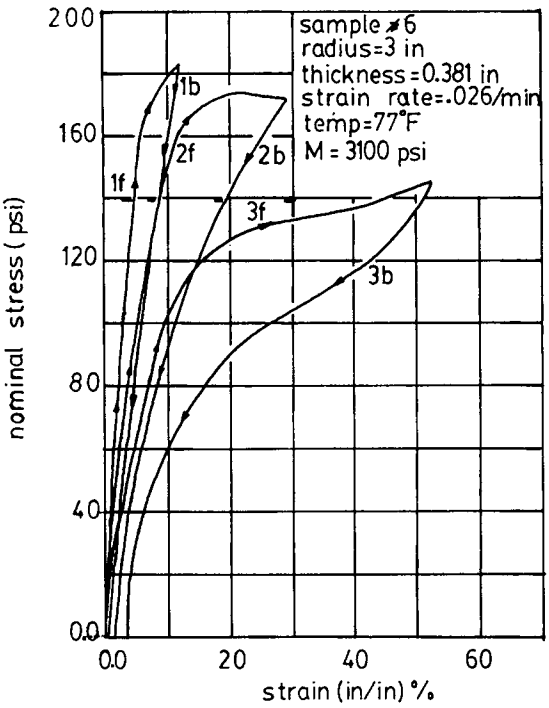

Figure 3 Stress–strain curve with hysteresis from a poker chip sample subjected to uniform tension.

MTS machine, up to 10% strain (path 1f), and returned to the undeformed state (path 1b) with the same speed as along the loading path. When the poker chip was pulled for the second time (path 2f) with the same speed as in path 1f, the material exhibited a *stress softening* (about 17% at 10% strain). Furthermore, when the sample was pulled for the third time, a further stress softening was observed. Tremendous *hysteresis* was also observed when the sample was returned to the undeformed state.

We attribute these two phenomena, i.e., the *stress softening* and the *hysteresis* to the opening and finally collapsing of existing voids within the tester poker-chip samples. Gent and co-workers[9] have also reported the existence of gas bubbles within rubber parts. It was shown[11] that the *viscoelasticity* does not play an important role for tests of low strain rate. Therefore, the *hysteresis* and the *stress softening* are due to the *voids*. These microvoids are formed within the poker chip along the curing of the samples. Hence, the number of gas bubbles which are formed within the material should be a function of the curing conditions. It was observed that, when the samples were cured for longer time, then the number of voids were drastically reduced within the samples.

It has been shown[6] that the apparent modulus M, of the poker chip with respect to the Young's modulus E of the material, is given via

$$\frac{M}{E} = \frac{1}{(1-2\nu)(1+\nu)}\left[(1-\nu) - \frac{2\nu^2}{(1-\nu)m - (1-2\nu)}\right] \quad (1)$$

where ν denotes Poisson's ratio and m is given by

$$m = \kappa a \frac{I_0(\kappa a)}{I_1(\kappa a)}, \qquad \kappa a = \frac{2a}{h}\sqrt{\frac{3-6\nu}{2-2\nu}} \quad (2)$$

where a and h denote the radius and the thickness of the poker chip sample. $I_0(\cdot)$ and $I_1(\cdot)$ are the modified Bessel functions.

By expanding the modified Bessel functions in a Taylor series and after some algebraic manipulations it can be proved that

$$\frac{M}{E} = 1 + \frac{3\nu^2}{1+\nu}\left(\frac{a}{h}\right)^2 - \frac{3\nu^2(7-6\nu)(1-2\nu)}{4(1+\nu)(1-\nu)}\left(\frac{a}{h}\right)^4 \quad (3)$$

Regarding the rubber as an incompressible solid ($\nu \cong 0.5$), eq. (3) becomes

$$\frac{M}{E} = 1 + \frac{1}{2}\left(\frac{a}{h}\right)^2 \quad (4)$$

Equation (4) is identical to Gent's equation.[3] For our experiments $a/h \approx 8$; hence, the theoretical value of $(M/E)_{th} = 33$.

From the stress–strain curve of the poker-chip sample (see Fig. 8) the apparent initial stiffness M was estimated to be approximately equal to $M \cong 21.374$ N/mm^2 (sample #6).

From the uniaxial tension experiments on 0-ring samples, it was found[11] that the Young's modulus of this material, whose chemical composition is given in Table I of Ref. (10), is equal to $E = 1.413$ N/mm^2. Hence the experimental value of $(M/E)_{exp}$ is equal to 15. Obviously, there is a difference between the experimental value and the theoretically predicted. We attribute this difference to the opening of *voids* within the deformed material.

STANDARD DEFINITION OF TERMS RELATING TO THE ACOUSTIC EMISSION

In this section, a number of definitions related to the acoustic emission technique are given. All the provided definitions of the acoustic emission terminology have been designated by the American Society for Testing and Materials (ASTM). *Transient elastic waves generated by the rapid release of energy from localized sources within a material are called acoustic emission.* Usually, terminologies as stress wave emission or just emission are often used in the literature. The number of times the acoustic emission signal exceeds a present threshold during any selected portion of a test is called *acoustic emission counts* N. The time rate at which acoustic emission counts occur is defined as the *acoustic emission count rate, or emission rate, or count rate,* $\dot{N}$.

A local material change giving rise to acoustic emission is called an *acoustic emission event.* The total elastic energy released by an emission event is called *acoustic emission event energy.* The peak voltage of the largest excursion attained by the signal wave from an emission event is called *acoustic emission signal.* The time interval between the detected arrivals of an acoustic wave at two different sensors is called the *arrival time interval* (Δt). The number of events with signals that exceed an arbitrary amplitute as a function of amplitute V, is defined as the *cumulative amplitude distribution,* $F(V)$. Also, we may define the *cumulative threshold crossing distribution* $F(V)$ as the number of times the acoustic emission signal exceeds an arbitrary threshold as a function of the threshold voltage. Figure 4 shows an acoustic emission event with the related definitions.

The acoustic emission signal is a transient phenomenon and the recorded signal may be compared to a dumped sinusoid. The most widely used method to process and quantify acoustic emission signals is *ringdown counting.* Before any test, a threshold value is assigned to eliminate the background noise. Usually, the threshold value has been assigned from the factory, for instance, 1 V. The number of threshold crossings is called *counts* and they are registered by a counter. For instance, in Figure 4 the counter will register 11 counts. The time from the first crossing of the threshold up to the last crossing is called the *duration* of an acoustic event. The time from the first crossing up to the crossing of the largest peak amplitude of the event is called *rise time*.

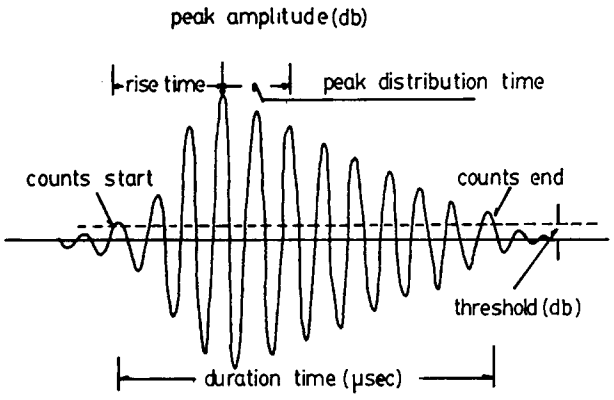

Figure 4 An acoustic emission event with related definitions.

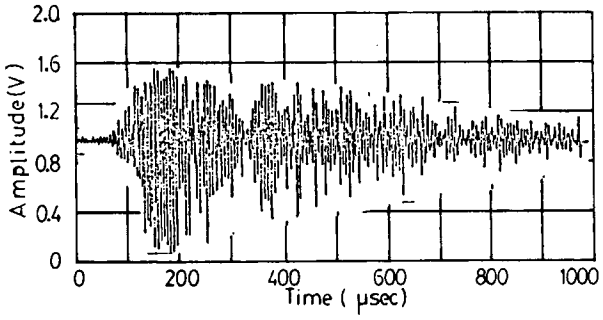

Figure 5 An acoustic emission event from a rubber poker chip sample subjected to tension.

ACOUSTIC EMISSION RESPONSE PULSES AND THEIR FREQUENCY SPECTRUM FROM A POKER-CHIP SAMPLE SUBJECTED TO UNIFORM TENSION

A typical experimental setup for the study of the growth and tearing microvoids in bonded rubber cylinders subjected to uniaxial tension is shown in Figure 4, of Ref. 10. In the last years, the acoustic emission pulses have been studied by a number of researchers.[12-15] Two types of emission have been observed. (1) *continuous-type emission,* which is primarily detected in metals, and (2) *burst-type emission,* which is mainly observed in composites, polymers and elastomers.

Figure 5 shows a typical acoustic emission signal from the poker chip samples whose chemical composition was depicted in Table I, of Ref. 10. The depicted AE purse was observed at large strain prior to rupture of the specimen. Obviously, this AE event has the same characteristics as the hypothetical signal of Figure 4 which represents a dumped oscillation. The *peak amplitude A* of the detected event is

approximately 1.5 V at the output of the sensors. It was observed that the peak amplitude of the AE events was increased as the strain increases too. At the present, we could not find a certain relationship between the peak amplitude and the deformation of the sample. The *duration time* t_D, and the *rise time* t_R are equal to 700 and 80 μs, respectively. We observed that the detected events along the tension tests had larger peak amplitude and longer duration and rise time in contrast to the events from the compression tests. This is readily understood because, along the tension of the specimen, the spherical growing voids collapse when the stress field around the void reaches a critical value. As a result of the tearing of the voids, a certain amount of energy is released which should be larger than the one released from the buckling of voids along the hydrostatic compression of the specimen.

The waveform of the emission carries information about the fine structure of the source event. Detailed interpretation of the wave forms is complicated by the occurrence of multiple reflections within the poker-chip specimen. These effects largely determine the waveform of the observed pulse and obscure the nature of the source waveform.

The frequency spectrum of the AE waveforms was analyzed (1) digitizing the transduced response and consequently performing a fast Fourier Transform (FFT) on the digitized pulse and (2) using a spectrum analyzer. Since the resolution of the second technique is not very good, the FFT technique was used in this study. The frequency analysis of the detected waveforms may yield information about the source event and the variations in the transmission properties of the material. One possible use of the frequency analysis is the detection of growing structural weakness and may be of initial stability. The frequency spectrum of the AE waveform of Figure 5 is depicted in Figure 6.

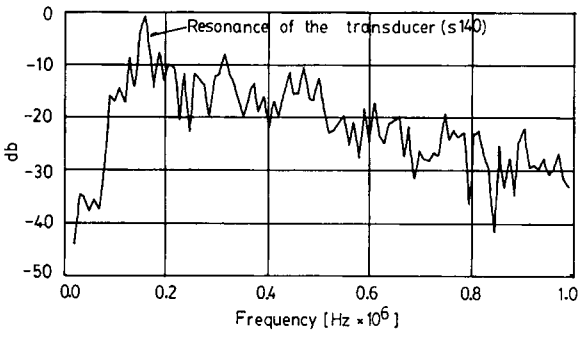

Figure 6 Frequency spectrum of the AE waveform of Figure 5.

Some strong peaks at 150 kHz and between 200 and 250 kHz are observed on the frequency spectrum of the AE waveform. The resonance of the sensor (Model S140) is 150 kHz; the remaining peaks are attributed to the frequency spectrum of the AE pulses.

Assuming that the collapse of the voids within the deformed elastomer may be approximated by an explosion in an infinite elastic medium then the displacement u_r at a distance r from the source is given via[16]

$$u_r = \frac{Pb}{\rho r^2}\psi(r, t)H[t - \kappa(r - b)] \tag{5}$$

where P defines the pressure at $r = b$, b and ρ are the radius of the void and the density of the elastomer, respectively, and $H[\cdot]$ is the step function. The parameter κ is defined via

$$\kappa^2 = \frac{\rho}{\lambda + 2\mu} \tag{6}$$

where λ and μ are the longitudinal and shear modulus of the medium, respectively.

The function $\psi(r, t)$ is given by

$$\psi(r, t) = e^{-\alpha[t-\kappa(r-b)]}\left\{\kappa r \cos(\omega[t - \kappa(r - b)] + \left(\frac{1 - \alpha\kappa r}{\omega}\right)\sin(\omega[t - \kappa(r - b)]\right\} \tag{7}$$

where the dumping coefficient α and the frequency ω of the transmitted acoustic wave is given by

$$\alpha = \frac{2\mu\kappa}{\rho b} \tag{8a}$$

$$\omega^2 = \frac{4\mu(\lambda + \mu)}{\rho(\lambda + 2\mu)b^2} \tag{8b}$$

It was found[11] that the modulus of elasticity for the testing rubber, whose chemical composition is given in Ref. 10, is equal to $E = 1.413$ n/mm^2. It was shown[17] that the effective Poisson's ratio for this material is $\nu_{ef} = 0.485$; therefore, the shear modulus μ is equal to 0.482 N/mm^2 and the longitudinal modulus λ is 8.687 N/mm^2. Assuming that the density of the rubber is almost 1 g/cm^3 and taken at $\omega \approx 300$ kHz, then eq. (8.2) yields the radius b of the voids being 900 μm. Equation (6) yields the value of κ equal to 4×10^{-5} s/cm. Substituting of b and

κ into eq. (8a), the dumping coefficient is equal to $\alpha = 4384\ s^{-1}$.

Hence, the acoustic emission can lead in a nondestructive experimental technique to the evaluation of the size of the voids within the sample. We could also estimate the size of the voids by cutting the samples after the test and magnifying these in an electron microscope. It was found that the size of the microvoids was about 1000 μm 15 of which are of the same order of magnitude as the one estimated from the AE data. The effects of voids on the response of rubber discs subjected to tension and the estimation of the initial voids content will be reported elsewhere.[17]

ACOUSTIC EMISSION BEHAVIOR OF AN UNFILLED NITRILE RUBBER DISC SUBJECTED TO UNIFORM TENSION

Along the tension of the poker chip samples a number of AE events were initially received at 6% strain and, thereafter, the received pulses were exponentially grown. The total number of the received AE events and the load applied on the poker-chip specimen as a function of the elapsed time of deformation is shown in Figure 7. The apparent modulus M of this sample was 15.513 N/mm^2, which is less than the modulus of sample #6. Obviously, this is due to smaller aspect ratio ($a \approx 6$) of sample #5. The number of received AE signals from the tension test is much bigger than the received from the compression of the specimen (see Ref. 10). The first AE pulses were received just before the yield point of the stress–strain curve. This observation was in general true for all the tested specimens. We also observed that the first events were located near the center of the tested poker chips. Change et al.[8] have also reported similar observations and furthermore that the voids

Figure 7 Total events and load vs. the elapsed time of deformation ($h \approx 1.27$ cm, $a = 7.62$ cm, V (piston) = 0.0254 in./min)

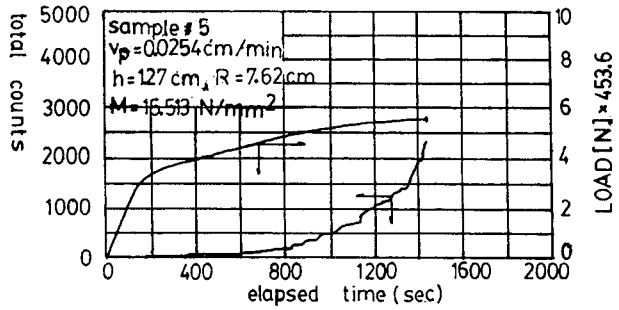

Figure 8 Total counts and load vs. the elapsed time of deformation (h = thickness, a = radius, V_p = speed of piston).

are located on circles whose centers coincide with that of the poker chip.

The total number of counts and the applied force as a function of the elapsed time is shown in Figure 8. The total number of the received counts (up to 45% strain) is approximately 2500. The window of the filter in the AE equipment was placed at 55 dB, in order to avoid the noise from the MTS machine. In some samples, we observed that a boundary failure occurred between the rubber and the steel plates. In this case, the samples were removed from the MTS machine and the received data were not taken in the account. The detected AE signals from the boundary failure were observed on the oscilloscope (after they were stored on a video recorder) which had a continuous type of form.

The event average rate E (or acoustic emission event rate) is shown in Figure 9. The total average count rate N is depicted in Figure 10. Both rate graphs indicate that most of the AE signals were depicted after the apparent yield point of the poker-chip sample.

The total number of counts $\sum N_i$ versus the applied force on the specimen is shown in Figure 11.

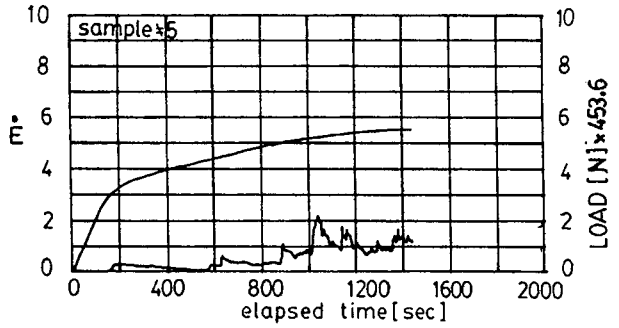

Figure 9 Event average rate $\dot{E}$ and load vs. time of deformation ($E = \Delta E/\Delta t$).

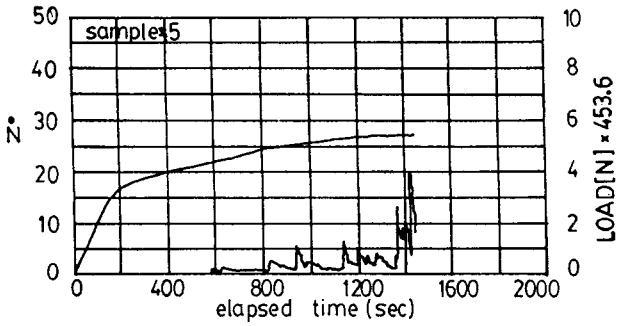

Figure 10 Total average count rate $\dot{N}$ and load vs. the time of deformation ($N = \Delta N/\Delta t$).

We observe that when the force is less than 900 N, the opening of voids within the material is negligible. This load corresponds to the apparent yield point on the stress–strain curve (see Fig. 7). In our view Figure 11 represents the best curve in order to prevent the internal damage of a testing material. A mathematical relation between the applied stress σ and the total number of detected AE counts N is given via the following equation[18].

$$N = Db\left[\sec\left(\frac{\pi\sigma}{2\sigma_1}\right) - 1\right] \tag{9}$$

where the material parameter D is a function of the strain rate, temperature, thickness, and microstructure, b denotes the size of the deformed voids, σ defines the applied stress, and σ_1 represents the stress where the rupture of the sample starts. The constant D can readily be determined by fitting the experimental data with eq. (9).

The normal amplitude distribution of the detected AE signals is shown in Figure 12. A wide distribution of the amplitude between 55 and 80 dB was observed. The threshold of the amplitude was specified at 50 dB in order to eliminate the noise from the MTS

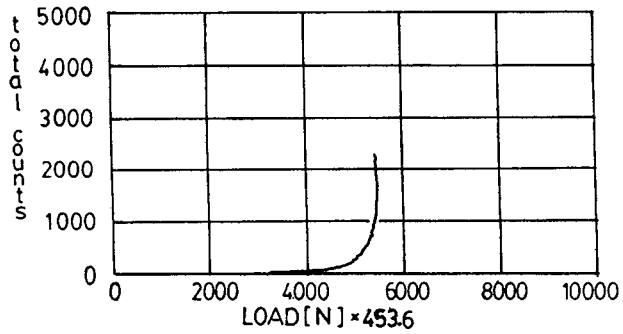

Figure 11 Total counts ΣN_i vs. applied load on the poker chip sample.

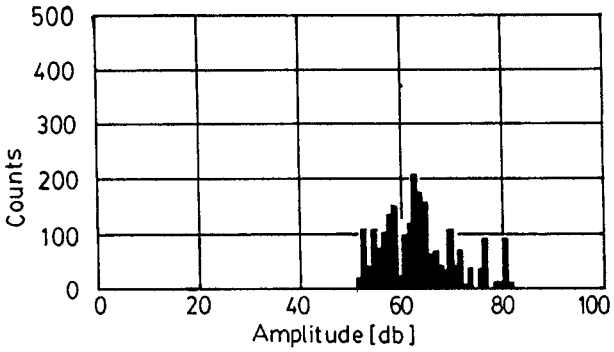

Figure 12 Normal amplitude distribution from the unfilled nitrile rubber poker-chip sample.

testing machine. Our experiences have shown that the Insron testing machine introduces less noise than the MTS machine. Hence, it is better to perform experiments on an Instron machine than an MTS. Unfortunately, the hydraulic system of the MTS introduces a tremendous noise. Since an amplitude of 0 dB corresponds to 1 μV at the source of the acoustic wave within the elastomer, Figure 12 indicates that most of the released AE waveforms had an amplitude between 0.35 and 10 mV.

CONCLUSIONS

It was shown that the drop of the apparent initial stiffness of a poker-chip elastomer sample subjected to uniform tension was due to the existence of voids within the testing material. From the frequency spectrum of the detected AE waveforms we extracted information about the size of the voids and the dumping coefficient of the elastomer material whose chemical composition was given elsewhere.[10,11] The total number of events and counts as a function of the elapsed time of deformation yield important information for the internal damage of the material under tension. As the material is deformed, the number of voids is exponentially increased. The total number of counts detected from the AE pulses increases drastically as the applied load is increased. The amplitude distribution of the received AE waveform yields information for the amplitude of the AE pulses at the source of the acoustic waveforms.

REFERENCES

1. M. L. Williams, in *Fracture of Solids*, Wiley-Interscience, New York, 1963.

2. A. N. Gent and P. B. Lindley, *J. Br. Rubber Producers Res. Assoc.*, **173,** 111 (1959).
3. A. N. Gent and P. B. Lindley, *Proc. Roy. Soc. (London)*, **249A,** 195 (1959).
4. G. H. Lindsey, R. A. Schaper, M. L. Williams, and A. R. Zak, Aerospace Research Laboratories Rept. ARL 63-152, 1963.
5. M. Levinson and P. J. Blatz, GALCIT SM 64-5, Cal. Inst. Tech., 1964.
6. M. L. Williams and R. Schapery, *Int. J. Fracture Mech.*, **1,** 64 (1965).
7. G. H. Lindsey, *J. Appl. Phys.*, **38**(12), 4843 (1967).
8. B. Wijayanta, W. V. Chang, and R. Salovey, *Rubber Chem. Techn.*, **51,** 1006 (1978).
9. A. Gent and D. Tompkins, *J. Appl. Phys.*, **40**(6), 2520 (1969).
10. P. A. Kakavas and W. V. Chang, *J. Appl. Polym. Sci.*, (1989) to appear.
11. P. A. Kakavas, Ph.D. dissertation, University of Southern California, Department of Chemical Engineering, 1987.
12. K. Ono and M. Yamamoto, *Mater. Sci. Eng.*, **47,** 247 (1981).
13. B. Betteridge et al., *Polymer*, **23,** 178 (1982).
14. I. Gradec, *J. Polym. Sci.*, **B12,** 573 (1974).
15. T. Brown, *Polym. News*, **8,** 263 (1982).
16. D. S. Berry, *J. Mech. Phys. Solids*, **6,** 177 (1958).
17. P. A. Kakavas and P. J. Blatz, *J. Appl. Polym. Sci.*, (1989) to appear.
18. B. J. Brindley, J. Holt, and I. G. Palmer, *Non-Destructive testing*, 299 (1973).

Received October 18, 1989
Accepted July 20, 1990